

Brain-Computer Interfaces for Detection and Localisation of Targets in Aerial Images

Ana Matran-Fernandez and Riccardo Poli

Abstract—Objective. The N2pc event-related potential (ERP) appears on the opposite side of the scalp with respect to the visual hemisphere where an object of interest is located. We explored the feasibility of using it to extract information on the spatial location of targets in aerial images shown by means of a rapid serial visual presentation (RSVP) protocol using single-trial classification. **Methods.** Images were shown to 11 participants at a presentation rate of 5 Hz while recording electroencephalographic signals. With the resulting ERPs we trained linear classifiers for single-trial detection of target presence and location. We analysed the classifiers' decisions and their raw output scores on independent test sets as well as the averages and voltage distributions of the ERPs. **Results.** The N2pc is elicited in RSVP presentation of complex images and can be recognised in single trials (the median area under the receiver operating characteristic curve was 0.76 for left vs right classification). Moreover, the peak amplitude of this ERP correlates with the horizontal position of the target within an image. The N2pc varies significantly depending on handedness, and these differences can be used for discriminating participants in terms of their preferred hand. **Conclusion and Significance.** The N2pc is elicited during RSVP presentation of real complex images and contains analogue information that can be used to roughly infer the horizontal position of targets. Furthermore, differences in the N2pc due to handedness should be taken into account when creating collaborative brain-computer interfaces.

Index Terms—Brain-computer interfaces, N2pc, P300, rapid serial visual presentation, handedness.

I. INTRODUCTION

Brain-Computer Interfaces (BCIs) convert signals from the brain into commands that allow users to control devices without relying on the usual peripheral pathways. Traditional BCIs aim at helping people with limitations in their motor control or their ability to communicate, such as those who are locked-in. Thus, typical BCI applications are spellers [1], [2], [3], wheelchair-control interfaces [4] or interfaces for computer mouse control [5], [6]. However, some forms of BCIs have recently started to be explored with the able-bodied population in mind, focusing on the augmentation of human capabilities [7] or the provision of a new means of control [8].

One of these new forms of BCIs focuses on augmenting human visual perception capabilities to speed up the process of finding pictures of interest in large collections of images [9],

Manuscript received XX. The early stages of this research were financially supported by the UK's Engineering and Physical Sciences Research Council (EPSRC). Grant EP/K004638/1, entitled "Global engagement with NASA JPL and ESA in Robotics, Brain Computer Interfaces, and Secure Adaptive Systems for Space Applications".

The authors would like to thank Dr Caterina Cinel for her useful comments on the manuscript and contributions to the early stages of the research.

The authors are with the Brain Computer Interfaces Laboratory, School of Computer Science and Electronic Engineering, University of Essex, UK. {amatra, rpoli}@essex.ac.uk

[10], [11], [12], [13], [14]. This problem is particularly important in counter intelligence and policing, where large numbers of images are screened in search for threats on a daily basis [13], [15]. However, other real-life applications of this technology include the screening of mammograms [16] and geoscientific images [17] by trained experts.

In these situations, typically, researchers use the Rapid Serial Visual Presentation (RSVP) protocol, in which sequences of images are shown at high presentation rates over a fixed area on the screen [18]. Observers are able to detect target configurations anywhere on the presentation area in the stream of images and these elicit distinct Event-Related Potentials (ERPs) in the electroencephalographic (EEG) signals acquired. In particular, if targets are reasonably rare, a P300 ERP (a large positive wave typically peaking 300–600 ms after stimulus onset) is likely to be produced in response to them as conditions are effectively those of the "oddball" paradigm [9], [19], [1].

Another ERP of particular interest for this work is the N2pc, which, in the literature, has predominantly been associated with selective attention processes [20], [21], [22], [23]. The N2pc is typically associated with the following interpretation: the first steps in perception are believed to be the automatic detection and coding of sensory features (e.g., shapes), followed by the first stage of attention shifting, known as *covert attention*, where people mentally shift their focus before/without moving their eyes [24], [25]. If participants are given a search template or a description of the target, the sensitivity of covert attention to objects/features that match this template is increased, so that they will be processed with higher priority. This shift of covert attention towards high priority areas is believed to be signalled by the N2pc [26].

Irrespective of what it represents, the N2pc is found in the presence of at least one distracting item (any non-target stimulus) apart from the target on the display [20]. It typically appears 170–300 ms after stimulus onset in contralateral electrode sites with respect to the visual hemifield where the target is located, presenting its maximum amplitude at electrodes PO7/PO8 and P7/P8 [26].

Only a few studies have considered the N2pc (on its own or together with other ERPs) for controlling a BCI [27], [28]. In [27], the authors found that N2pc components can help identify popout targets accurately (but with large variations in classification accuracy across participants) when averaging signals acquired over three repetitions of stimulus presentation. Moreover, the N2pc was used together with the P300 ERP to control a BCI for communication by a disabled participant in [28], achieving a classification accuracy of 80%. The authors also tested this paradigm with healthy users for

other applications, such as control of a robot and Internet browsing, achieving perfect classification after 6 repetitions of the stimuli.

In this paper, we explore the feasibility of using the N2pc to extract information on the spatial location of targets in stimuli representing complex real-life scenes for a task of practical utility (aerial image sifting) presented using an RSVP protocol through BCIs based on single-trial classification. This is an exceptionally difficult task for a BCI as: (1) the N2pc is a much smaller ERP than the P300 in terms of voltage amplitudes, duration and locations where it can be detected, (2) we use a single-trial approach, and (3) we use a rapid presentation rate. To moderate these difficulties we used a presentation rate at the lower end of the spectrum for RSVP (namely, 5 Hz) and restricted the target template to a specific airplane (albeit with variable rotations and positions).

We hypothesise that, if the N2pc can be detected in such a scenario, it could be exploited, for example, to help circumscribe the area of the image where the target is located, thereby speeding up the job of the person reviewing the potential targets detected by a BCI. Also, it could help improve target detection if, for instance, targets too lateral with respect to an observer's gaze to cause a fully blown P300 still cause a detectable shift of attention resulting in an N2pc. To verify these hypotheses, we also investigated the relative dependency of target classification on the P300 and the N2pc.¹

We should note that our approach is different from the one used in many other RSVP-based BCI systems for target detection where participants are required to press a key when they see a target (sometimes called the behavioural task) [9], [10], [31], [13], [14], [32], [33], and then use only the trials in which the target was correctly identified by the participant (e.g., by including only those trials that were followed by a key press within a pre-defined time period) when plotting grand averages and for training a classifier with clean data. However, this method has several drawbacks [11], including variations in reaction times (RTs) depending on task difficulty, presentation rates and other factors, and *artefact contamination in the EEG resulting from the keypress*. For these reasons, we decided against such an approach.

The organisation of this paper is as follows. Section II describes the experimental setup used for data collection and the signal processing techniques that were applied to these data. Section III presents the results of our experiments. We will start by focusing on the detection of targets in our experiment by means of the P300. Next, as little to no information is available in the literature in relation to whether and at what

sites the N2pc is elicited in conditions remotely similar to those adopted in this work, we will explore whether the N2pc component is present in the EEG signals recorded from our experiment by means of an ERP analysis. We will then study whether (and to what extent) a classification system based on linear Support Vector Machines (SVMs) takes advantage of the information provided by this (lateralised) component for target detection. Finally, we will look at the degree to which the N2pc can be used to estimate the position of a target within the field of view and study the differences in this ERP that arise as a consequence of participant's handedness. We discuss our findings in section IV and provide conclusions in section V. Possible avenues for future work will also be considered in these two sections.

II. METHODS

A. Participants and setup

We gathered data from 11 volunteers with normal or corrected-to-normal vision (mean \pm SD = 24.5 \pm 3.83 years old, four females, five left-handed). They all read, understood and signed an informed consent form approved by the Ethics Committee of the University of Essex.

Participants were seated at approximately 80 cm from the LCD screen where the stimuli were presented. EEG data were acquired with a BioSemi ActiveTwo system with 64 electrodes following the international 10-20 system, plus one electrode on each earlobe. The EEG was referenced to the mean of the electrodes placed on the earlobes. The initial sampling rate was 2048 Hz. Signals were band-pass filtered between 0.15 and 28 Hz with a non-causal FIR filter obtained by convolving a low-pass filter with a high-pass filter, both designed with the window method. Data were then downsampled to 64 Hz before correcting for eye blinks and ocular movements. This was performed by applying the standard subtraction algorithm based on correlations to the average of the differences between channels Fp1-F1, and Fp2-F2 [34].

B. Experimental design

The images for our experiments consisted of 2,400 aerial pictures of London. All images were converted to grayscale and their histograms were equalised. Picture size was 640 \times 640 px² (thus subtending a visual angle of 11.5 \times 11.8 degrees), and pictures were centred on the middle of the LCD screen. Target (T) pictures were aerial pictures in which a randomly rotated and positioned airplane had been (photo-realistically) superimposed (see breakout in Fig. 1). Non-target (NT) images did not contain airplanes.

Pictures were shown to participants in sequences (or bursts) of 100 images which were presented at a rate of 5 Hz, with no gaps between two consecutive stimuli as illustrated in Fig. 1. Each burst lasted 20 seconds and was preceded by a fixation cross for 1 second. Ten target pictures were randomly inserted within each sequence (the remaining 90 being non-targets) with the only restriction that there had to be at least one NT image between two target ones. The ratio of target vs non-target images was 10%.

¹The work presented in this paper branches out of preliminary research where we experimented with collaborative BCIs (cBCIs) for the classification of aerial images where the outputs of two [29] and three [12] individually-trained classifiers were averaged in order to improve classification performance. In [30] we also checked the presence of the N2pc ERP for different presentation rates and created a 2-person cBCI for target localisation. The stimulation protocol and a subset of the participants used for this study were originally tested in such prior work. However, that work did not study the ERPs themselves through single-channel grand averages or scalp maps, did not look at raw classifier-scores and their distributions, did not look at the issue of predicting the fine-grain location of targets via N2pc and it did not look at differences in the N2pc based on handedness — all of which we have done here.

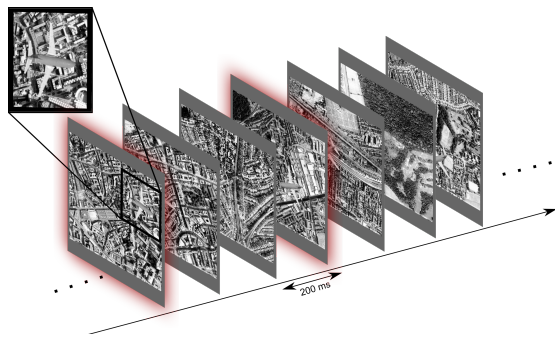


Fig. 1. Illustration of the protocol used in our experiments. Images containing a target were randomly interspersed within a stream of non-target images. For clarity, target images are highlighted in this figure.

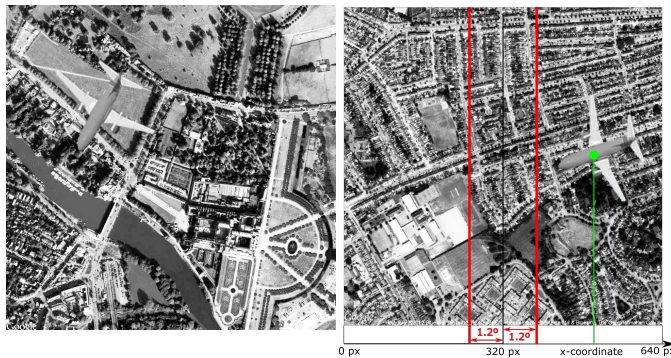


Fig. 2. Example of LVF (left) and RVF (right) target images used in the experiment. The parameters of the stimuli have been superimposed on the RVF target image.

To enhance the amplitude of the P300 [35], participants were assigned the task of mentally counting the planes they saw within each burst and report the total at the end of a burst (to encourage them to stay focused on the task). Participants could rest after bursts and were free to decide when to start the next burst (by clicking on a mouse button).

C. Lateral targets

Approximately 60% (144 out of 240) of our target images contained a lateral target (i.e., the target appeared on the left or right side of the picture). More specifically, we had 59 Left Visual Field (LVF) target pictures and 85 Right Visual Field (RVF) target pictures.²

The coordinate of the airplane was established as the x -coordinate of the centroid of the plane. The origin of x -coordinates was located on the lower left corner of the image, as shown in Fig. 2(right). A target was considered to be lateral if it was positioned at a visual angle ≥ 1.2 degrees on the horizontal axis (with respect to the centre of the screen). Examples of an LVF and an RVF target can be seen in Fig. 2.

As we will discuss later, the epochs associated with these images were analysed with particular attention, as such images were expected to generate N2pc as well as P300 ERPs.

²The imbalance in the cardinality of the LVF and RVF target sets is due to a slight undetected bias in the algorithm that was used to position the planes. This was, however, inconsequential other than it slightly reduced the statistical significance of some of our findings.

TABLE I
MAIN FEATURES OF THE DATASETS USED IN OUR STUDY. SEE TEXT FOR MORE DETAILS.

Objective	#trials for training*		#trials for testing*		#folds
	Class 1	Class 2	Class 1	Class 2	
<i>T vs NT classification</i>	216	1944	24	216	10
<i>LVF vs RVF classification</i>	53	76	6	9	10
<i>Target localisation</i>	780 (LH) or 936 (RH)		420 (LH) or 504 (RH)		1
<i>LH vs RH classification</i>	340 or 425	510 or 425	85 or 0	0 or 85	11

*In each cross-validation fold.

D. Feature selection and classification

We expected both the P300 and the N2pc ERPs to be rarer (or have a reduced amplitude) in response to non-targets than in the case of targets. Also, we did not expect them to be always present together even for targets. Given the differences in their known characteristics, we used different sets of features in order to best detect and exploit each ERP. These will be described below in two corresponding sections.

It is common in BCIs to average signals from several trials in order to increase the signal-to-noise ratio of ERPs and improve classification performance. Averaging would slow down our systems, thereby significantly reducing the range of applications for which they could be utilised. For this reason, in this work we will make single-trial decisions for *classification* purposes. We will, however, make use of grand averages for the *analysis of ERPs* as is customary in BCI, psychophysiology and neuroscience.

In the following subsections we will describe four uses of our experimental data, each characterised by a different choice of training and test sets. Table I summarises such choices to help readers keep track of these differences.

1) *Detection of the P300 component*: We expected the classification of target and non-target images to rely mostly on the P300 ERP,³ but we wanted to see to what degree the N2pc could influence it. We extracted epochs that contained the 300–600 ms interval after stimulus onset. This resulted in a total of 20 features per electrode.

In an effort to reduce the total number of features used for the task and minimise the risk of overfitting, we used only centro-posterior-occipital electrode sites as these are typically where P300s are most prominent. In one combination (E_{28}) we used 28 electrodes (see Fig. 3). The second combination (of 20 electrodes, E_{20}) was identical to the first except that we omitted electrode sites where the N2pc is most prominent according to the literature. A third combination (E_{24}) included the electrodes in E_{20} plus four electrode differences particularly suitable for the detection of the N2pc (see next section). So, for the purpose of classification, epochs were represented with between 400 and 560 features. As before, epochs were referenced to the average voltage in the 200 ms interval before stimulus onset.

For each participant, we used 10-fold stratified cross-validation to train an ensemble of two hard-margin linear SVM classifiers. The training set of each fold was used itself to

³Unless otherwise stated, in this article, whenever we refer to the P300 we intend the positive posterior ERP also known in the literature as P3b [35] and not the earlier more-frontal ERP known as P3a [36].

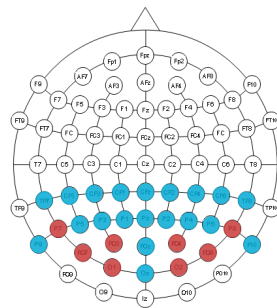


Fig. 3. Electrodes used for the different classification tasks. Electrodes in blue represent the E_{20} combination. All the highlighted electrodes were used in the E_{28} combination. Differences between pairs of electrodes in red were used for the detection of the N2pc. Combination E_{24} included the blue electrodes plus the differences of electrodes used for the N2pc.

find the optimal C parameter (i.e., the misclassification cost, $C \in \{10^{-8}, 10^{-7}, \dots, 1\}$) of the classifiers via 10-fold cross-validation. Each classifier was trained to distinguish between the T and NT conditions. The optimised ensemble for each participant was tested on the epochs from the independent test set.

We recorded the analogue output scores of the SVMs, with which we then computed the Receiver Operating Characteristic (ROC) curve for each participant. This indicates the balance between sensitivity and specificity of a classifier obtained when a control parameter (typically a threshold) is changed. Following an established standard, we condensed the information contained in each ROC curve into a single performance figure: the Area Under the Curve (AUC) [37], [38]. The closer the AUC to 1, the better the classifier. Although there are no general guidelines, classification systems are considered acceptable when their AUC is higher than 0.7 [39]. In BCI applications, a threshold of 0.8 is typically used in order to obtain a level of performance that guarantees that the time that it takes to output a symbol (including corrections to errors made by the system) will not be too long to discourage users (e.g., [40], [41]).

2) *Detection of the N2pc component:* To verify whether we could detect the N2pc component in single trials in the conditions of our experiment, we extracted epochs of EEG signal from approximately 200 ms to 400 ms after stimulus onset (the temporal window where the N2pc most often occurs according to the literature). This resulted in 14 samples per channel at the 64 Hz sampling rate used. The data were referenced to the mean value of the 200 ms interval before stimulus onset.

Since the N2pc is a lateralised ERP, it is more easily revealed when looking at *differences* between pairs of electrodes corresponding to symmetric positions with respect to the brain’s median plane than when processing left and right electrodes independently. Furthermore, it is most prominent in the posterior and occipital electrodes. Based on this, when detecting N2pc components in our experiments we used the set of four differences between electrode pairs: (PO7–PO8), (P7–P8), (PO3–PO4) and (O1–O2) (see Fig. 3). Concatenating these electrode differences yields a feature-vector repre-

sentation of epochs including $14 \times 4 = 56$ elements.

With this input representation, we performed 10-fold stratified cross-validation to train an ensemble of two hard-margin linear SVM classifiers to distinguish between LVF and RVF targets from our set of 144 lateral target pictures. Again, the training fold was itself used internally to optimise the misclassification cost of the ensemble via 10-fold cross-validation, and the performance of the classifiers was measured via the AUC.

3) *Target localisation:* We hypothesised that the N2pc could be used to tell to what degree a target is lateral with respect to the centre of the image. In order to test this hypothesis, we used a linear predictor which was optimised by a Particle Swarm Optimiser (PSO) [42]. The representation used in the PSO included 17 parameters: eight were interpreted as indices in the 56-dimensional feature vector extracted from each epoch (see Section II-D2), another eight were the coefficients for the corresponding features, and one was a constant term for the linear predictor. The fitness function optimised by the PSO was multi-objective as we aimed at: (1) obtaining a correlation, $\rho_{\text{predictor}}$, between actual outputs and desired outputs (the x coordinate of the target, in pixels, in the picture corresponding to each epoch) as close as possible to the correlation, $\rho_{\text{reference}}$, obtained by a standard linear regressor using all the features, and (2) ensuring the regression line between the desired outputs and the outputs of our linear predictor has as a slope close as possible to 1.⁴ Formally, the fitness function (to be minimised) was:

$$f = |1 - \text{slope}|^2 + |\rho_{\text{reference}} - \rho_{\text{predictor}}| + 0.0005 \times \text{MAE}$$

where *slope* and MAE are the slope and the mean absolute error of the linear regression between the desired outputs and the outputs of our linear predictor, respectively.

The PSO was trained using a random split of 65% of *all target* trials for either all left-handed or all right-handed volunteers, and tested on the remaining trials from the group. Thus, for the former we had 780 training samples (240 trials/participant \times 5 participants \times 65%), and 420 test samples, whereas for the latter the number of training and testing samples were 936 and 504, respectively.

We separated the participants into left- and right-handed groups due to differences found in the N2pc depending on the handedness of the volunteers (more on this below).

4) *Handedness detection:* Finally, we trained linear SVM classifiers to perform discrimination of left-handed (LH) vs right-handed (RH) participants. We performed 11-fold leave-one-participant-out cross-validation. In each fold, after training, all the trials from the training set for both classes (each one represented by the RVF target epochs for either left- or right-handed participants) were fed to the classifiers, and the median output score was computed. This value was used as a threshold for comparing the median output score for the excluded participant and classify him/her as LH or RH.

⁴We used this approach to compensate for the tendency of standard multivariate regression to compress its output range in the presence of strong noise on its inputs.

III. RESULTS

In this section we will present the results of our experiments. More specifically, in Section III-A we will look at grand averages and scalp maps indicating the presence and timing of the P300 and N2pc ERPs in our data, while in Section III-B we will report on the performance of our BCIs for T vs NT and LVF vs RVF classification. Finally, in Section III-C we consider differences in perception of lateral targets depending on the handedness of the participant. Based on these differences, we study the degree to which a linear predictor can be used to quantify the eccentricity of a target with respect to the centre of the image.

A. Analysis of ERPs

Before we look at the ERPs obtained in our experiments, we should note that, as is common in other BCIs such as the matrix speller [1], [43], when using very short stimulus onset asynchrony (SOA), ERPs are significantly deformed with respect to their “textbook” form found in electrophysiology and neuropsychology studies (e.g., see [44]). For instance, in our RSVP experiment, EEG signals contain a large SSVEP component at the frequency of stimulation (5 Hz) due to the involuntary response of the visual system. However, as we will see below, this waveform is modulated by the ERPs selectively generated by different stimuli.

1) *P300*: Let us start by looking at the grand averages of the ERPs for the T and NT conditions. These, together with their difference, are shown in Fig. 4 (left) for electrode site Pz, while the scalps in Fig. 4 (right) show the grand-averaged spatial distributions at 297 and 515 ms after stimulus onset.

Due to the above-mentioned SSVEP modulation, there appear to be two peaks on the difference waveform of Fig. 4 (left), one at about 300 ms and a second one around 600 ms, both referred to stimulus onset. However, this double peak, which is also present in the grand average waveform for the target trials, should not appear on the P3b [35], [45], [46]. We thus believe that the pronounced decrease is due to this SSVEP modulation, whose effects are also manifested in the scalp maps reported on Fig. 4 (right).

To see if the observed peak differences were statistically significant, we defined the peak amplitude of the P3’ as the mean voltage amplitude in the time intervals 300–400 ms after stimulus onset, and the peak amplitude of the P3” as the mean voltage amplitude 500–600 ms after stimulus onset for T and NT trials. We applied a Kruskal-Wallis test (a one-way, non-parametric, analysis-of-variance test) [47], [48] to test for differences between the T and NT conditions for electrode sites Cz, CPz and Pz for both peaks. We found that all such differences are highly significant at the tested electrodes (p values $< 3 \times 10^{-4}$) except for the P3” amplitudes in Cz, which are not statistically different.

2) *N2pc*: To verify the presence of the N2pc ERP, in Fig. 5 we show grand averages for lateral targets. The “contralateral” line in the figure represents the grand average of participant averages that were computed by averaging the epochs recorded from channel PO7 (on the posterior-occipital *left* region of the scalp) for all RVF targets with the epochs recorded from

channel PO8 (on the posterior-occipital *right* region of the scalp) for all LVF targets. Similarly, the “ipsilateral” line represents grand averages where we averaged the epochs recorded from channel PO7 for LVF targets with the epochs recorded from channel PO8 for all RVF targets. We adopted these ipsilateral and contralateral grand averages, following the conventions of the N2pc literature, as these emphasise left-right asymmetries that would otherwise be lost with standard averages. Following the same conventions, we plotted these data using an *inverted ordinate axis* (so higher means more negative). To further illustrate the differences between the two conditions, in the figure we also report the difference between the contralateral and ipsilateral grand averages (line labelled as “N2pc”).

As we can see from the figure, the ipsilateral and contralateral ERPs start to deviate markedly from each other at 250 ms after stimulus onset, with their difference peaking at approximately 340 ms. The shape and sign of the deflection is consistent with those of the N2pc reported in the literature, even though in our experiment its latency was slightly longer than in other studies, presumably because attention (both covert and overt) is also attracted (and, thus, divided) by features of the constant stream of distractors (non-targets) used in our experiments⁵.

Fig. 6 shows snapshots of the temporal evolution of the grand averages across the scalp between approximately 310 ms and 375 ms after the presentation of images containing a lateral target. Looking at the grand averages for LVF targets (top), the voltages at several contralateral posterior and occipital electrodes (e.g., PO4, PO8, P8) start becoming more negative than those in corresponding ipsilateral channels (e.g., PO3, PO7, P7) from around 300 ms after stimulus onset. This difference increases over time. The same effect can be observed in the grand averages for RVF targets (bottom), where the voltages at left posterior electrodes (i.e., the contralateral channels) are more negative than the corresponding voltages of the right (i.e., ipsilateral) channels in the same time interval⁶.

This figure shows a pattern of activation in the frontal lateral electrodes (e.g., FT7, FT8), showing that there are eye movements in the horizontal axis in response to lateral targets. However, their amplitude is much smaller than that shown in Fig. 5, so the horizontal component of the electrooculogram alone cannot account for the differences observed.

We measured the N2pc “peak” amplitudes (computed as the mean value of the voltage difference between pairs of contralateral and ipsilateral electrodes in the time interval 280–380 ms after stimulus onset) for LVF and RVF targets. The medians of these amplitudes across all participants and trials are reported in Table II for electrode differences *PO7–PO8*, *P7–P8*, *PO3–PO4* and *O1–O2*. The table also reports the p values obtained from the Kruskal-Wallis test applied to these data. As one can see, the voltage asymmetries we documented

⁵Unfortunately, there is not enough information in the literature to know whether the filters used in each article are causal or not, and, thus, it is not possible to ascertain whether the differences in latency are due to our non-causal filter [49] or to the different paradigm used in this work.

⁶Of course, there are asymmetries of brain function in the left and right hemispheres and, so, we cannot expect perfectly symmetric scalp maps.

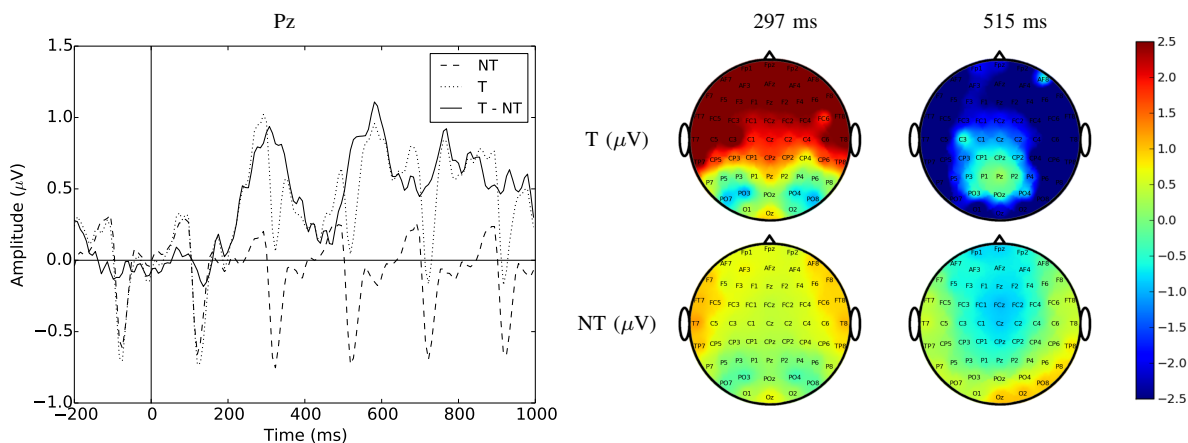


Fig. 4. Stimulus-locked grand averages for T and NT trials at channel Pz and their differences (left) and scalp maps of the grand averages for T and NT at 297 ms and 515 ms after stimulus onset.

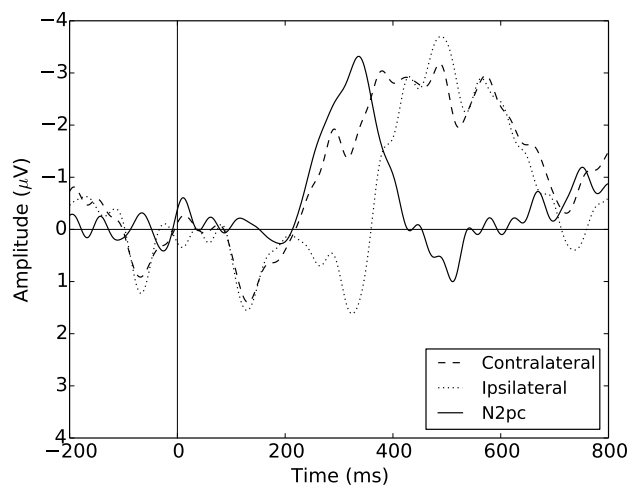


Fig. 5. Contralateral and ipsilateral stimulus-locked grand averages at channels PO7 and PO8 and their difference (continuous line) across lateral targets from the training set.

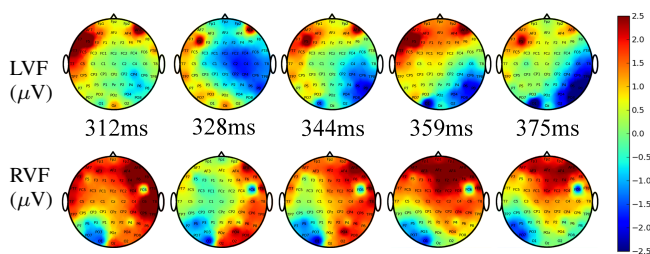


Fig. 6. Grand-averaged ERP scalp distributions between 312 ms and 375 ms after the onset of LVF (top row) and RVF targets (bottom row).

in these channels where the N2pc is typically found are highly statistically significant.

B. Single-trial classification

In this section we will look at the performance and behaviour of the two BCIs considered in this work: one for the classification of T vs NT images and one for the classification of LVF vs RVF for images that are already known to contain a target.

TABLE II
MEDIAN AND KRUSKAL-WALLIS p VALUES FOR THE PEAK AMPLITUDES OF THE VOLTAGE DIFFERENCES BETWEEN CONTRALATERAL AND IPSILATERAL CHANNELS FOR LVF AND RVF TARGETS.

Electrode difference	N2pc: median peak amplitude		p value
	LVF	RVF	
$PO7 - PO8$	1.646 μV	-1.950 μV	2.2×10^{-16}
$P7 - P8$	1.897 μV	-1.301 μV	8.5×10^{-10}
$PO3 - PO4$	1.559 μV	-1.813 μV	3.3×10^{-16}
$O1 - O2$	0.868 μV	-0.902 μV	1.2×10^{-4}

1) *Target vs non-target classification*: As described in section II-D1, for the classification of T vs NT trials we tested several different combinations of electrodes: one basic combination of centro-parietal electrodes where the P300 ERP is most prominent (E_{28}), a second one that did not include those electrodes that were used for the detection of the N2pc (E_{20}), and finally a third combination (E_{24}) that used the features from the electrodes in combination E_{20} plus the four pairs of electrode differences used for N2pc detection. We obtained median AUC values of 0.873, 0.856 and 0.858, respectively. A one-sided paired Wilcoxon rank test comparing the participant-by-participant results revealed that the small difference in medians for combinations E_{28} and E_{20} is statistically significant (p value= 7×10^{-3}), as is the difference between combinations E_{28} and E_{24} (p value= 7×10^{-3}). This confirms that there is a consistent, albeit small, advantage in integrating channels where the N2pc is typically present with those where P300s are most prominent for the purpose of detecting targets. However, comparisons between E_{20} and E_{24} (p value=0.5) revealed no statistically significant differences.

Moreover, the median Information Transfer Rate (ITR) across all folds and participants for the T vs NT classification task in the E_{28} configuration, using the entropy formula [50] was 41.03 bpm.

To gain more information about the reliance of the T vs NT classifiers on the N2pc and their behaviour in the presence of different types of stimuli, we estimated the probability density functions (pdfs) for the SVM output scores obtained for T vs NT classification using the E_{28} and E_{20} electrode combinations. Since we wanted to distinguish between the

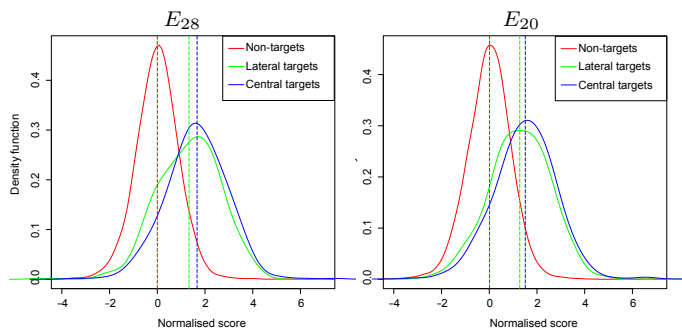


Fig. 7. Probability density functions of the SVM normalised scores in the T vs NT classification for non-targets, lateral targets and central targets using combinations E_{28} (left) and E_{20} (right) electrodes, computed via R’s Gaussian-kernel-based density estimator. Vertical lines represent the mean of each distribution.

cases where an N2pc is expected from those where it is unlikely to be elicited, we computed separate (conditional) pdfs for lateral and central targets as well as the (total) pdf for all non-targets. Fig. 7 shows the results. To provide a common reference and make it possible to appreciate relative differences between classes, the pdfs were normalised by subtracting the mean of the non-target scores and were then scaled by the standard deviation of the same class (so the non-target pdf has zero mean and unitary standard deviation).

As shown in the figure, the pdfs for targets and non-targets are reasonably well separated (as also highlighted by our earlier AUC analysis). However, both for E_{28} and E_{20} we see that the pdfs for central and lateral targets differ to some degree, with the central targets achieving higher scores than the lateral targets (approximately 1.67 vs 1.33 for E_{28} and 1.50 vs 1.27 for E_{20} , respectively). To verify if these differences are statistically significant, we performed a one-sided Mann-Whitney test to compare the medians of these distributions across participants [51], [52]. The results show that the score shifts of lateral targets with respect to central ones are highly statistically significant for combinations E_{28} (p value = 3.9×10^{-5}), E_{20} (p value = 0.001) and E_{24} (p value = 0.002).

As we discussed in section II-C, we expected that P300s would be different for lateral targets than for central ones. The observed shift in the distributions for lateral targets is likely to be a manifestation of this.

2) *LVF vs RVF classification*: As shown in Section III-A2, there are marked asymmetries in the posterior-occipital lateral regions of the scalp in the interval 200–400 ms after stimulus presentation when comparing the ERPs generated by lateral targets. We, therefore, expected that the four electrode differences listed in Section II-D2 when computed in this interval would allow an SVM classifier to distinguish between LVF and RVF lateral targets. The mean and standard deviations of the AUCs across all folds for each participant can be seen in Table III.

This table shows, consistently with the literature [27], that there are large variations in performance across participants, with AUCs ranging between 0.67–0.88. Notably, the AUC median, 0.76, is reasonably high, which is very encouraging

TABLE III
MEAN AND STANDARD DEVIATIONS OF THE AUC VALUES OBTAINED FOR LVF VS RVF CLASSIFICATION FOR EACH PARTICIPANT, ACROSS ALL FOLDS.

Participant	AUC (Mean \pm standard deviation)
1	0.75 \pm 0.13
2	0.88 \pm 0.07
3	0.81 \pm 0.17
4	0.81 \pm 0.08
5	0.81 \pm 0.11
6	0.76 \pm 0.17
7	0.67 \pm 0.17
8	0.71 \pm 0.17
9	0.80 \pm 0.16
10	0.67 \pm 0.16
11	0.70 \pm 0.13
Median	0.76

considering the amplitude of the N2pc and the small scalp regions where the it can be detected.

If we now divide *all* targets into left and right targets according to whether their centroid falls in one or another half of the image, rather than following the visual angle convention described in section II-C, we can calculate the ITR of the system as if it was a 3-class problem in the following scenario. Each trial was first passed to the T vs NT classifier. If this first system labelled it as an instance of class T, then it was passed to the LVF vs RVF classifier. This resulted in three classes: LVF target, RVF target and non-target. Using this approach, we obtained a median ITR of 49.73 bpm. A paired one-sided Wilcoxon signed-rank test comparing the participant-by-participant ITRs for the two-class (see Section III-B1) vs the three-class scenarios showed that this difference is not statistically significant (p value = 0.05).

C. Target Localisation, Handedness and the N2pc

After initially trying to predict target localisation and obtaining promising results, we noticed some differences in the ERPs produced by left- and right-handed participants⁷. Given the approximate balance between LH and RH individuals in our pool of participants, we then started to look at the differences in the N2pc ERP in the two groups, finding important differences.

1) *Target localisation*: Fig. 8 (left) shows the contralateral minus ipsilateral grand averages across all lateral targets for LH and RH participants. This plot also shows the p values from a one-sided Mann-Whitney test comparing ERP amplitudes over time. As shown, there are highly significant differences between the N2pc in LH and RH participants (i.e., values of p above the horizontal line), especially in the tail of the ERP in the time window 280–400 ms after the onset of the stimuli.

The scalp maps shown in the right side of Fig. 8 highlight the spatial differences between left- and right-handed participants when observing LVF (top) and RVF targets (bottom).

⁷By “handedness” we refer to the self-reported handedness of the participants in the study. More specifically, we asked volunteers to tell us their preferred hand for writing. Since we did not expect there would be implications of our study on handedness research, we did not perform the standard tests that are routinely used to more objectively verify the handedness of participants.

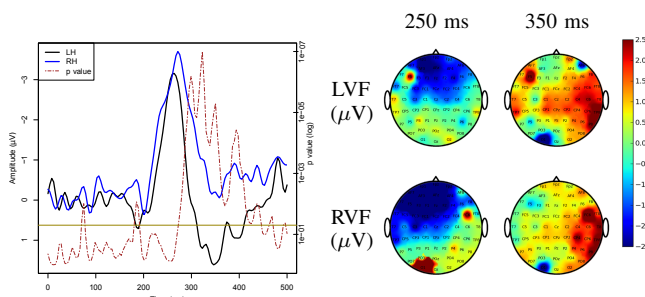


Fig. 8. Left: Contralateral minus ipsilateral stimulus-locked grand averages for LH and RH participants across all lateral targets, and p values from a one-sided Mann-Whitney test comparing both conditions. Values of p above the horizontal line are statistically significant at the 5% level. Right: difference scalp maps between left- and right-handed individuals of the grand averages for LRVF (top) and RVF (bottom) targets.

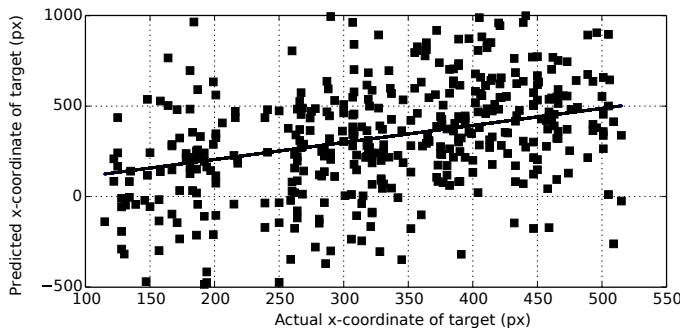


Fig. 9. Predicted x-coordinate for the target vs actual target position (in pixels) for all target images in the test set (lateral or not), using only LH participants. The regression line is also shown.

Given the differences in the N2pc depending on handedness, we decided to separate groups of users depending on their self-reported preferred hand when training the PSO predictor. Moreover, since the differences across the left- and right-handed groups were greater in the set of RVF targets, we also chose to use only this set to classify between left- and right-handed people.

As hypothesised, the amplitude of the N2pc can also be used to determine the distance of the target from the centre of the picture. Fig. 9 shows the coordinates of the target output by our PSO-optimised linear predictor (trained as explained in Section II-D3) vs the actual coordinates of the target for the group of left-handed participants. A similar plot (not reported) was obtained for RH participants. In all cases, the eight features selected by the PSO represent the amplitude of the N2pc in electrode differences between PO7-PO8, P7-P8 and PO3-PO4.

The correlation between the predictor’s output and the actual x-coordinate of the target on the test set for this group is $\rho=0.42$ (and $\rho=0.39$ for the RH group). These correlations are significantly higher than those obtained individually by each participant, showing that there is an advantage in using the collaborative approach when trying to locate a target within an image.

2) *Handedness classification:* Finally, in terms of left- vs right-handed classification (LH vs RH), we achieved a classification accuracy of 100% with the method described in

Section II-D4, showing that there is information in the N2pc that can be used to discriminate participants in terms of their preferred hand.

Considering that there are quicker alternatives to assess the handedness of a participant (e.g., the Edinburgh Handedness Inventory test [53]), we are *not* suggesting the use of our RSVP-BCI method to determine whether a participant is left- or right-handed. Rather, we want to point out that the differences in the N2pc due to handedness should be taken into account when working with this component. This applies to collaborative BCIs, especially if EEG signals from the individuals that compose a group are averaged directly [12], but also when doing grand averages and studies of attention.

IV. DISCUSSION

One of the objectives of our experiments was to understand whether the N2pc ERP was present during rapid presentation of real-world images by means of our RSVP paradigm.

Results indicate that the N2pc is evoked and can reliably be detected in the conditions of our experiments. For instance, we were able to obtain a median AUC value of 0.76 for single-trial LRVF vs RVF classification (i.e., based on N2pc detection), with the top quartile of our participants showing AUCs of 0.81 or above. This range of AUCs is typically considered to be acceptable in the field of BCI. We also found that the form of the N2pc that is elicited in response to lateral targets differs for RH and LH participants. By analysing the correlation between horizontal position and scores, we revealed that the N2pc can not only be used to distinguish between LRVF and RVF targets, but it can also tell to what degree a target is lateral.

Our ERP analysis also revealed that the N2pc components evoked using our paradigm had a greater latency than has previously been reported in the literature. In part, this may be due to the greater complexity of the stimuli used in our study in comparison to the simple stimuli traditionally used in the literature. However, we suspect that the stimulus presentation technique we used (i.e., RSVP) is the prominent reason for the greater latency. In typical N2pc-evoking experiments, participants are shown an array of objects or symbols either for a short amount of time (usually <300 ms) with a generous inter-stimulus interval (>1.5 s), or until they find the target. However, in the RSVP paradigm of our experiment, images follow each other very quickly, and, thus, a target image is immediately followed by one or more non-targets. We hypothesise that these effectively act as masks for the target picture, thus resulting in a significant increase in the cognitive load of the task and in diverting attentional resources away from it. Because of this, in our in our experiments the N2pc precedes the P300 by less than in other setups.

RSVP-based BCIs pose a very attractive alternative for the development of gaze-independent systems that are suitable for severely locked-in people with no gaze control [54], [55], [28]. Thus, we believe that the study presented can help improve BCIs aimed at communication systems by the disabled, e.g., by investigating whether the explicit use of the N2pc can help determine which column the user is focusing on. Moreover, the fact that the N2pc is present in people with no gaze

control makes them suitable to operate systems such as the one presented in this work, thus potentially increasing their employability.

An advantage of using the RSVP protocol for controlling a BCI is the capability to increase the ITR of the system, which is another reason why these systems are particularly interesting in applications of BCI for disabled people. Moreover, we have shown in this work that we can increase the ITR of our system by dividing the “target” class into two subclasses, depending on the laterality of the target, even if the left vs right classification task is performed after a trial has been classified by the T vs NT system as a target (i.e., we have a sequential system).

We also showed that differences in the N2pc due to handedness can effectively be used to discriminate between left- and right-handed participants. We did not perform a handedness test on our volunteers, and as such, these results should be taken as a preliminary result. Although there is previous evidence of the dependence between handedness and memory [56], handedness and brain morphology [57], [58] and EEG signals being different depending on handedness [59], to the best of our knowledge, these differences have not been exploited to assess the handedness (or preferred hand) of a person.⁸ As we said in Section III-C2, we do not believe that our method to determine the handedness of a person should be instead of the already existing ones. The important message behind our result is the fact that the differences found due to handedness should be taken into account in studies based on this ERP, such as those that use the N2pc as a marker of attention shifts, which are currently mostly based on right-handed participants.

This same suggestion applies to the field of collaborative BCIs, specially in the case where the (raw or pre-processed) EEG signals are directly averaged across multiple users. Just as different latencies of a given ERP extracted from several participants affect (possibly decreasing) the performance of the BCI trained from those signals, the same might happen if there are differences in the ERPs that arise from the handedness of the participant. This is a matter that people in the field of collaborative BCI should take into account and which might be useful to create high performance systems.

In our analysis of ERPs and classifier outputs in the T vs NT classification task, we found that targets produce significant P300 components that are not present in the non-targets, making the classes even better separable than in the LVF vs RVF task. We showed that the raw outputs of the T vs NT classifiers are (statistically significantly) smaller for lateral targets than for central ones, suggesting that a link between P300 and eccentricity exists in our setup. While the difference is small compared with the that between targets and non-targets, it still means that the BCI misses more lateral targets than central ones. Symmetrically, the LVF vs RVF classifier

selectively responds to lateral targets with a clear negative or positive response, but does not respond (producing a near-zero score) for central targets and, in preliminary tests, also non-targets.

All of these effects suggest that there could be ways of exploiting handedness and lateralisation (as emphasised by the N2pc) to build even better performing integrated T vs NT and LVF vs RVF classification systems. Further radical improvements in these systems can also be obtained by integrating neural evidence from multiple observers to improve the accuracy of classification systems, as we did in [12], [29]. We will explore both these research avenues in the future.

V. CONCLUSIONS

In this paper, we looked at the possibility of exploiting the P300 and N2pc ERPs in a BCI which automatically detects targets in aerial pictures of urban environments and one that approximately establishes the horizontal position of the target within pictures known to contain one. To the best of our knowledge, this is the first attempt to analyse and exploit the N2pc with stimuli representing complex real-life scenes and for a task of real practical utility.

Our classification results for target detection are aligned with results obtained by equivalent single-trial BCIs utilising RSVP protocols at our rate of presentation. Interestingly, however, the results of LVF vs RVF classification based on the N2pc electrode-sites and time-window are also very encouraging, producing a median AUC of almost 0.80.

By studying the N2pc ERP, we have been able to find a significant correlation between its features (as represented by this ERP’s amplitude and time course) and the horizontal position of targets within images, which suggests a whole spectrum of possible BCI applications for this ERP in the future. Finally, we also showed differences in the N2pc due to participant’s self-reported preferred hand, which can be useful for other studies that rely on this component, and for cBCIs.

REFERENCES

- [1] L. Farwell and E. Donchin, “Talking off the top of your head: toward a mental prosthesis utilizing event-related brain potentials,” *Electroencephalography and Clinical Neurophysiology*, vol. 70, no. 6, pp. 510–523, 1988.
- [2] R. Scherer and G. Muller, “An asynchronously controlled EEG-based virtual keyboard: improvement of the spelling rate,” *IEEE Transactions on Biomedical Engineering*, vol. 51, no. 6, pp. 979–984, 2004.
- [3] J. R. Wolpaw et al, “Brain-computer interfaces for communication and control,” *Clinical Neurophysiology*, vol. 113, no. 6, pp. 767–791, 2002.
- [4] F. Galán et al, “A brain-actuated wheelchair: asynchronous and non-invasive brain-computer interfaces for continuous control of robots,” *Clinical Neurophysiology*, vol. 119, no. 9, pp. 2159–2169, 2008.
- [5] F. Beverina et al, “User adaptive BCIs: SSVEP and P300 based interfaces,” *PsychNology Journal*, vol. 1, no. 4, pp. 331–354, 2003.
- [6] L. Citi et al, “P300-based BCI mouse with genetically-optimized analogue control,” *IEEE Transactions on Neural Systems and Rehabilitation Engineering*, vol. 16, no. 1, pp. 51–61, Feb. 2008.
- [7] E. B. Coffey et al, “Brain-machine interfaces in space: using spontaneous rather than intentionally generated brain signals,” *Acta Astronautica*, vol. 67, no. 1, pp. 1–11, 2010.
- [8] R. Poli et al, “Towards cooperative brain-computer interfaces for space navigation,” in *Proceedings of the 2013 International Conference on Intelligent User Interfaces*. ACM, 2013, pp. 149–160.
- [9] A. D. Gerson et al, “Cortically coupled computer vision for rapid image search,” *IEEE Transactions on Neural Systems and Rehabilitation Engineering*, vol. 14, no. 2, pp. 174–179, Jun. 2006.

⁸The only article that we are aware of that touches upon this subject is [60]. However, we felt that there are a number of flaws in the methodologies and inconsistencies in the results, including setting the threshold for classification based on the test data, contradictions in whether or not the participants from the second experiment (whose results are never reported) were left-handed, and forgetting to include the results claimed in (their) Section 4.5.

- [10] L. Parra et al., "Spatiotemporal linear decoding of brain state," *IEEE Signal Processing Magazine*, no. January 2008, pp. 107–115, 2008.
- [11] P. Sajda et al., "In a Blink of an Eye and a Switch of a Transistor: Cortically Coupled Computer Vision," *Proceedings of the IEEE*, vol. 98, no. 3, pp. 462–478, Mar. 2010.
- [12] A. Matran-Fernandez et al., "Collaborative brain-computer interfaces for the automatic classification of images," in *Neural Engineering (NER), 2013 6th International IEEE/EMBS Conference on*. San Diego (CA): IEEE, 6–8 November 2013, pp. 1096–1099.
- [13] A. R. Marathe et al., "The effect of target and non-target similarity on neural classification performance: A boost from confidence," *Frontiers in Neuroscience*, vol. 9, no. 270, 2015.
- [14] H. Cecotti et al., "Optimization of single-trial detection of event-related potentials through artificial trials," *IEEE Transactions on Biomedical Engineering*, vol. 62, no. 9, 2015.
- [15] Y. Huang et al., "A framework for rapid visual image search using single-trial brain evoked responses," *Neurocomputing*, vol. 74, no. 12, pp. 2041–2051, 2011.
- [16] C. Hope et al., "High throughput screening for mammography using a human-computer interface with rapid serial visual presentation (RSVP)," in *SPIE Medical Imaging*. International Society for Optics and Photonics, 2013, pp. 867303–867303.
- [17] Y. Sivarajah et al., "Quantifying target spotting performances with complex geoscientific imagery using ERP P300 responses," *International Journal of Human-Computer Studies*, 2013.
- [18] K. Forster, "Visual perception of rapidly presented word sequences of varying complexity," *Perception & Psychophysics*, vol. 8, no. 4, pp. 215–221, 1970.
- [19] N. K. Squires et al., "Two varieties of long-latency positive waves evoked by unpredictable auditory stimuli in man," *Electroencephalography and clinical neurophysiology*, vol. 38, no. 4, pp. 387–401, 1975.
- [20] S. J. Luck and S. A. Hillyard, "Spatial filtering during visual search: evidence from human electrophysiology," *Journal of Experimental Psychology: Human Perception and Performance*, vol. 20, no. 5, pp. 1000–1014, 1994.
- [21] M. Eimer, "The N2pc component as an indicator of attentional selectivity," *Electroencephalography and Clinical Neurophysiology*, vol. 99, no. 3, pp. 225–234, 1996.
- [22] M. Kiss et al., "The N2pc component and its links to attention shifts and spatially selective visual processing," *Psychophysiology*, vol. 45, no. 2, pp. 240–249, 2008.
- [23] C. Hickey et al., "Electrophysiological evidence of the capture of visual attention," *Journal of Cognitive Neuroscience*, vol. 18, no. 4, pp. 604–613, 2006.
- [24] A. M. Treisman, "Strategies and models of selective attention," *Psychological review*, vol. 76, no. 3, p. 282, 1969.
- [25] C. Koch and S. Ullman, "Shifts in selective visual attention: towards the underlying neural circuitry," in *Matters of Intelligence*. Springer, 1987, pp. 115–141.
- [26] S. Luck, "Electrophysiological correlates of the focusing of attention within complex visual scenes: N2pc and related ERP components," *Oxford Handbook of ERP components*, 2012.
- [27] H. Awani et al., "Towards a brain computer interface based on the N2pc event-related potential," in *6th Annual International IEEE EMBS Conference on Neural Engineering*. San Diego (CA): IEEE, 6–8 November 2013.
- [28] J. S. Blasco et al., "Visual evoked potential-based brain-machine interface applications to assist disabled people," *Expert Systems with Applications*, vol. 39, no. 9, pp. 7908 – 7918, 2012.
- [29] A. Stoica et al., "Multi-brain fusion and applications to intelligence analysis," in *Proceedings of SPIE Volume 8756*, Baltimore, Maryland, USA, 30 April – 1 May 2013.
- [30] A. Matran-Fernandez and R. Poli, "Collaborative Brain-Computer Interfaces for Target Localisation in Rapid Serial Visual Presentation," in *Computer Science and Electronic Engineering Conference (CEEC), 2014 6th*. IEEE, 2014, pp. 127–132.
- [31] A. D. Gerson et al., "Cortical origins of response time variability during rapid discrimination of visual objects," *Neuroimage*, vol. 28, no. 2, pp. 342–353, 2005.
- [32] J. Touryan et al., "Estimating endogenous changes in task performance from EEG," *Frontiers in Neuroscience*, vol. 8, 2014.
- [33] A. R. Marathe et al., "Confidence metrics improve human-autonomy integration," in *Proceedings of the 2014 ACM/IEEE international conference on Human-robot interaction*. ACM, 2014, pp. 240–241.
- [34] P. Quilter et al., "The removal of eye movement artefact from EEG signals using correlation techniques," in *Random Signal Analysis, IEEE Conference Publication*, vol. 159, 1977, pp. 93–100.
- [35] J. Polich, "Neuropsychology of P3a and P3b: a theoretical overview," *Brainwaves and mind: Recent developments*, pp. 15–29, 2004.
- [36] M. D. Comerchero and J. Polich, "P3a, perceptual distinctiveness, and stimulus modality," *Cognitive Brain Research*, vol. 7, pp. 41–48, 1998.
- [37] J. Hanley and B. McNeil, "The meaning and use of the area under a receiver operating characteristic (ROC) curve," *Radiology*, vol. 143, pp. 29–36, 1982.
- [38] A. P. Bradley, "The use of the area under the ROC curve in the evaluation of machine learning algorithms," *Pattern Recognition*, vol. 30, no. 7, pp. 1145–1159, 1997.
- [39] J. A. Swets, "Measuring the accuracy of diagnostic systems," *Science*, vol. 240, no. 4857, pp. 1285–1293, 1988.
- [40] M. Schreuder et al., "Optimizing event-related potential based brain-computer interfaces: a systematic evaluation of dynamic stopping methods," *Journal of Neural Engineering*, vol. 10, no. 3, p. 036025, 2013.
- [41] I. Daly et al., "Brain computer interface control via functional connectivity dynamics," *Pattern Recognition*, vol. 45, no. 6, pp. 2123–2136, 2012.
- [42] R. Poli et al., "Particle swarm optimization," *Swarm intelligence*, vol. 1, no. 1, pp. 33–57, 2007.
- [43] C. Cinel et al., "Possible sources of perceptual errors in P300-based speller paradigm," *Biomedizinische technik*, vol. 49, pp. 39–40, 2004, Proceedings of 2nd International BCI workshop and Training Course.
- [44] S. J. Luck, *An introduction to the event-related potential technique*. Cambridge, Massachusetts: MIT Press, 2005.
- [45] J. Polich, "Updating P300: an integrative theory of P3a and P3b," *Clinical neurophysiology*, vol. 118, no. 10, pp. 2128–2148, Oct 2007.
- [46] G. McCarthy and E. Donchin, "A metric for thought: a comparison of P300 latency and reaction time," *Science (New York, N.Y.)*, vol. 211, no. 4477, pp. 77–80, Jan 1981.
- [47] W. H. Kruskal and W. A. Wallis, "Use of ranks in one-criterion variance analysis," *Journal of the American Statistical Association*, vol. 47, no. 260, pp. 583–621, 1952.
- [48] A. Kübler et al., "Brain-computer communication: Self-regulation of slow cortical potentials for verbal communication," *Archives of Physical Medicine and Rehabilitation*, vol. 82, no. 11, pp. 1533 – 1539, 2001.
- [49] A. Widmann and E. Schröger, "Filter effects and filter artifacts in the analysis of electrophysiological data," *Frontiers in Psychology*, vol. 3, p. 233, 2012.
- [50] A. Schlögl, C. Keinrath, R. Scherer, and G. Pfurtscheller, "Information transfer of an EEG-based brain computer interface," in *Proceedings of the 1st International IEEE EMBS Conference on Neural Engineering*, 2003, pp. 641–644.
- [51] H. B. Mann and D. R. Whitney, "On a test of whether one of two random variables is stochastically larger than the other," *The annals of mathematical statistics*, pp. 50–60, 1947.
- [52] C. Guger et al., "How many people are able to control a p300-based braincomputer interface (BCI)?" *Neuroscience Letters*, vol. 462, no. 1, pp. 94 – 98, 2009.
- [53] R. C. Oldfield, "The assessment and analysis of handedness: the Edinburgh inventory," *Neuropsychologia*, vol. 9, no. 1, pp. 97–113, 1971.
- [54] L. Acqualagna and B. Blankertz, "Gaze-independent BCI-spelling using rapid serial visual presentation (RSVP)," *Clinical Neurophysiology*, vol. 124, no. 5, pp. 901–908, 2013.
- [55] M. S. Treder et al., "Gaze-independent brain-computer interfaces based on covert attention and feature attention," *Journal of Neural Engineering*, vol. 8, no. 6, p. 066003, 2011.
- [56] K. B. Lyle et al., "Handedness is related to memory via hemispheric interaction: evidence from paired associate recall and source memory tasks," *Neuropsychology*, vol. 22, no. 4, p. 523, 2008.
- [57] M. Habib et al., "Effects of handedness and sex on the morphology of the corpus callosum: A study with brain magnetic resonance imaging," *Brain and Cognition*, vol. 16, no. 1, pp. 41 – 61, 1991.
- [58] S. F. Witelson, "The brain connection: the corpus callosum is larger in left-handers," *Science*, vol. 229, no. 4714, pp. 665–668, 1985.
- [59] T. Nielsen et al., "Interhemispheric EEG coherence during sleep and wakefulness in left-and right-handed subjects," *Brain and Cognition*, vol. 14, no. 1, pp. 113–125, 1990.
- [60] C. A. Ng and W. Leong, "An EEG-based approach for left-handedness detection," *Biomedical Signal Processing and Control*, vol. 10, pp. 92 – 101, 2014.